ACS APPLIED MATERIALS & INTERFACES

Research Article

www.acsami.org

Enhanced Thermoelectric Performance of PEDOT:PSS Flexible Bulky Papers by Treatment with Secondary Dopants

Desalegn A. Mengistie,[†,‡,§] Chang-Hsiao Chen,[∥] Karunakara M. Boopathi,[†,‡,⊥] Ferry W. Pranoto,[∥] Lain-Jong Li,[∥] and Chih-Wei Chu*[,‡,#]

[†]Nanoscience and Technology Program, Taiwan International Graduate Program, [‡]Research Center for Applied Sciences, and [∥]Institute of Atomic and Molecular Sciences, Academia Sinica, Taipei 115, Taiwan

[§]Bahir Dar University, Bahir Dar, P.O. Box 26, Ethiopia

[⊥]Department of Engineering and System Science, National Tsing Hua University, Hsinchu 30013, Taiwan

[#]Department of Photonics, National Chiao Tung University, Hsinchu 30010, Taiwan

Supporting Information

ABSTRACT: For inorganic thermoelectric materials, Seebeck coefficient and electrical conductivity are interdependent, and hence optimization of thermoelectric performance is challenging. In this work we show that thermoelectric performance of PEDOT:PSS can be enhanced by greatly improving its electrical conductivity in contrast to inorganic thermoelectric materials. Free-standing flexible and smooth PEDOT:PSS bulky papers were prepared using vacuum-assisted filtration. The electrical conductivity was enhanced to 640, 800, 1300, and 1900 S cm^{-1} by treating PEDOT:PSS with ethylene glycol, polyethylene glycol, methanol, and formic acid, respectively. The Seebeck coefficient did not show significant variation with the tremendous conductivity enhancement being 21.4 and 20.6 $\mu V\ K^{-1}$ for ethylene glycol- and formic acid-treated papers, respectively. This is because secondary dopants, which increase electrical conductivity, do not change oxidation level of PEDOT. A maximum power factor of 80.6 $\mu W\ m^{-1}\ K^{-2}$ was shown for formic acid-treated samples, while it was only 29.3 $\mu W\ m^{-1}\ K^{-2}$ for ethylene glycol treatment. Coupled with intrinsically low thermal conductivity of PEDOT:PSS, ZT ≈ 0.32 was measured at room temperature using Harman method. We investigated the reasons behind the greatly enhanced thermoelectric performance.

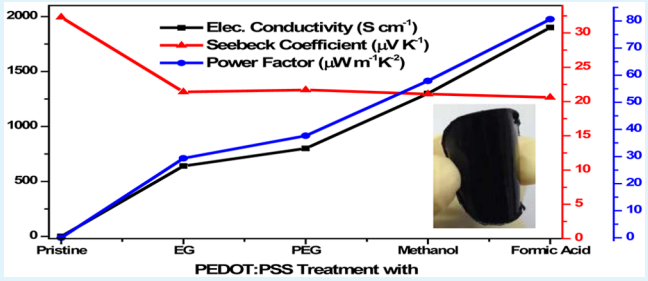

KEYWORDS: *PEDOT:PSS, conductivity enhancement, flexible thermoelectrics, Seebeck coefficient, power factor, conductive polymer*

1. INTRODUCTION

Thermoelectric (TE) materials directly convert natural or waste heat into pollution-free electricity or vice versa. Our planet has ubiquitous heat sources; from solar heat to industrial or vehicle exhausts, which are essentially free, that could be converted into electricity using TEs. The interesting features of TE generators are ease of switching between power generation mode (based on the Seebeck effect) and cooling mode (based on the Peltier effect), no moving parts, no fluid involved, silent, and high reliability.[1,2] Widespread use of TEs requires improving the performance of the materials as well as implementing them in system architecture. The performance of TE materials is measured by a dimensionless figure-of-merit, $ZT = S^2\sigma T/\kappa$; where S, σ, T, and κ are Seebeck coefficient (also called thermopower), electrical conductivity, absolute temperature, and thermal conductivity, respectively. There is interdependence between the three parameters σ, κ, and S, and they must be fine-tuned simultaneously to optimize ZT.[3] The defining parameters behind them are carrier concentration, effective mass of charge carriers, and the electronic and lattice thermal conductivities. This interdependent property is a challenge for materials selection as materials that are good electrical conductors are also good thermal conductors and show low Seebeck coefficients.

The best-performing TE materials are inorganic semiconductor alloys, complex crystals, and nanocomposites or thin film superlattices such as Bi_2Te_3, PbTe, BiSb, Bi_2Se_3 MgSi, $CoSb_3$, $NaCo_2O_4$, etc.[4,5] The highest ZT value reported is ∼2.4 at room temperature for p-type Bi_2Te_3/Sb_2Te_3 superlattice devices.[6] However, the inorganic TE materials are posed with drawbacks of energy-intensive high-temperature processing, high cost of production, brittleness, and difficulty in large-area production, scarcity of materials, and toxicity. A TE power generator device consists of semiconductor legs that are connected electrically in series and thermally in parallel covering large area and different shapes. This in turn requires TE materials that are readily synthesized, air stable, environ-

Received: February 17, 2014
Accepted: December 5, 2014
Published: December 5, 2014

DOI: 10.1021/am507032e
ACS Appl. Mater. Interfaces 2015, 7, 94−100

mentally friendly, and solution-processable to create patterns on large areas.

Organic or polymer-based semiconductors/conductors are emerging and potential TE materials that will offer several advantages such as mechanical flexibility, low cost, lightweight, and solution processability over large areas even though their efficiency is much lower than the inorganic counterparts.[7−10] The intrinsically low thermal conductivity of organic materials, which is ∼2 to 3 orders of magnitude lower than those of the inorganics, makes them potential candidates for high-performance TE applications. Polymeric TE materials investigated include poly(thienothiophene),[11] polyaniline,[12] poly(3,4-ethylenedioxythiophene) (PEDOT),[13] polyacetylene,[14] and poly(3-hexylthiophene).[15] Among them, PEDOT doped with a counterion polymer poly(styrenesulfonate) (PSS) is highly promising and showed ZT ≈ 0.42 at room temperature optimized by tuning the doping/dedoping level.[16] The theoretical simulation even indicates that the TE performance of PEDOT:PSS can rival high-efficiency inorganic TE materials.[17]

PEDOT:PSS, commercially available in aqueous dispersion, is a successful conductive polymer for optoelectronics applications.[18−20] Through continuous efforts, its conductivity has been increased to over 3400 S cm^{-1}, and it has been used as transparent electrode for polymer solar cells and organic light-emitting diodes.[21,22] Conductivity enhancement of PEDOT:PSS has been effective through mixing of high boiling point polar solvents like ethylene glycol (EG), dimethyl sulfoxide, ionic liquids, etc. into the aqueous PEDOT:PSS dispersion,[23−25] film post-treatment with polar solvents, alcohols, acids, or cosolvents[26] or a combination of both treatment methods.[27] These treatment chemicals used to enhance the conductivity are generally called secondary dopants, which are apparently "inert" substances that induce further conductivity enhancement and other property changes. The newly enhanced properties remain even after complete removal of the secondary dopant.[28] Unlike the inorganic TE materials, electrical conductivity enhancement in PEDOT:PSS affects very little the Seebeck coefficient and thermal conductivity.[16,29] In PEDOT:PSS, only small crystallites are embedded in the amorphous phase, and hence the thermal conductivity will show only slight variation with conductivity enhancement.[30] Because of its inherent low thermal conductivity, improvement of TE performance of PEDOT:PSS focuses on improvement of its power factor ($S^2\sigma$).

In this work, we show that the TE performance of PEDOT:PSS flexible bulky papers is enhanced by enhancing the electrical conductivity. The conductivity of the papers, which were prepared by facile method, was enhanced to 1900 S cm^{-1} using different treatment methods. As the conductivity enhancement methods we employed do not change the oxidation level of PEDOT, the Seebeck coefficient decreased only slightly with improving conductivity being 33.2 and 20.6 μV K^{-1} for pristine and formic acid-treated papers, respectively. The highest power factor obtained is 80.6 μW m^{-1} K^{-2} for formic acid-treated papers. A ZT value ≈ 0.32 was measured using Harman method.

2. EXPERIMENTAL SECTION

2.1. Preparation and Characterization of PEDOT:PSS Bulky Papers. PEDOT:PSS aqueous solution (Clevios PH1000) with concentration of 1.0−1.3% by weight and 2.5 weight ratio of PSS to PEDOT was used. Both thin film (∼200 nm) and bulky papers (∼100 μm) were prepared. Thin films were prepared on glass substrates with area 1.5 × 1.5 cm^2 by spin coating multiple times until the desired film thickness is obtained. Treatment with EG, PEG (polyethylene glycol with molecular weight 200), methanol, and formic acid (FA, >98% v/v) was done as reported in our previous works.[31−33] Briefly, 6% EG and 2% PEG200 were mixed in the PEDOT:PSS aqueous solution before spin coating, while methanol and FA treatment was done by treating the annealed films. Flexible bulky papers were prepared with the aid of vacuum-assisted filtration using the setup shown in Figure S1 (Supporting Information). Anodisc filter membrane (Whatman, 0.2 μm pore size with 47 mm diameter) was used as a filter. In vacuum filtration, the liquid is sucked down through the filter membrane by the action of water pump leading to greater rate of filtration compared to gravity filtration. Since the vacuum pulls down the liquid, it is possible to get thick papers in a short period of time. Filtration was continued for 3 h with water pump, and then the samples were dried under vacuum oven at 40 °C for 3 h. Drying could also be done in atmospheric oven, but it was difficult to peel the filter membrane from the paper in the latter case. Then annealing was continued on a hot plate for ∼10 min at 140 °C. Methanol and FA treatment was done by dropping ∼600 μL of either of them on the paper while annealing with optional treatment/rinsing with methanol and DI water thereafter, respectively.

Film thickness was measured using alpha step surface profiler (Veeco Dektak 150). Electrical conductivities were measured using van der Pauw four-point probe technique with Hall Effect measurement system (Ecopia, HMS-5000). Absorption spectra of the films were measured using Jacobs V-670 UV−vis-NIR spectrophotometer. X-ray photoelectron spectroscopy (XPS) was done using PHI 5000 VersaProbe (ULVAC-PHI, Chigasaki, Japan) equipped with Al Kα X-ray source (1486.6 eV). Surface morphologies of the films/papers were imaged using an atomic force microscope (AFM) (Veeco di Innova) in the tapping mode. Raman spectra were collected in a confocal Raman system (NT-MDT). The wavelength of laser was 473 nm (2.63 eV), and the spot size of the laser beam was ∼0.5 μm with a 10 s accumulation time. The X-ray diffraction (XRD) patterns of the bulky papers were obtained using PANalytical XRD.

2.2. Seebeck Coefficient Measurement. The Seebeck coefficient was measured using a homemade setup (Figure 1b), which consisted of two Peltier devices attached on a copper-covered aluminum heat sink. Two K-type thermocouples were used to measure the temperature gradient across the samples. The thermocouples and the two probes used to measure the voltage difference (ΔV) were applied at the same point on the paper/film and pressed with Teflon bar against the film to make a good contact. This minimizes the error that will come during measurement. The gap between the thermocouples was ∼5 mm. Agilent 34401A attached to copper foil probe (∼5 mm wide) was used to measure ΔV. The hot side of the Peltier was heated with applied current of ∼0.5 A continuously using power supply (TECPEL TPT 3025) resulting in a temperature gradient (ΔK) of ∼10−15 K, and reading of the values (ΔV and ΔK) was taken after ∼3 min to let the values stabilize. The values were then averaged by taking ∼five consecutive readings. The Seebeck coefficient was calculated using the formula $S = \Delta V/\Delta T$.

2.3. ZT Measurement by Harman Method. The transient Harman method was used for the measurement of the in-plane and vertical ZT of TE materials at room temperature using the setup shown in Figure S2 (Supporting Information). The Harman method consists of passing a direct current using a power supply (Keithley 2400) through a thermoelectric sample and measuring the voltage drop using oscilloscope. The total voltage drop that could be generated across the sample is composed of resistive voltage V_R and thermoelectric voltage (Seebeck voltage, V_S). The temperature difference across the sample is induced by Peltier effects between both ends of material. Once the current is switched off, V_R instantaneously drops to 0, and the remaining V_S decays gradually as the sample returns to thermal equilibrium with the ambient. The platinum electrodes cover the whole surface of both ends of the sample, so that the current streamline will be parallel to the longitudinal axis of the sample.

DOI: 10.1021/am507032e
ACS Appl. Mater. Interfaces 2015, 7, 94−100

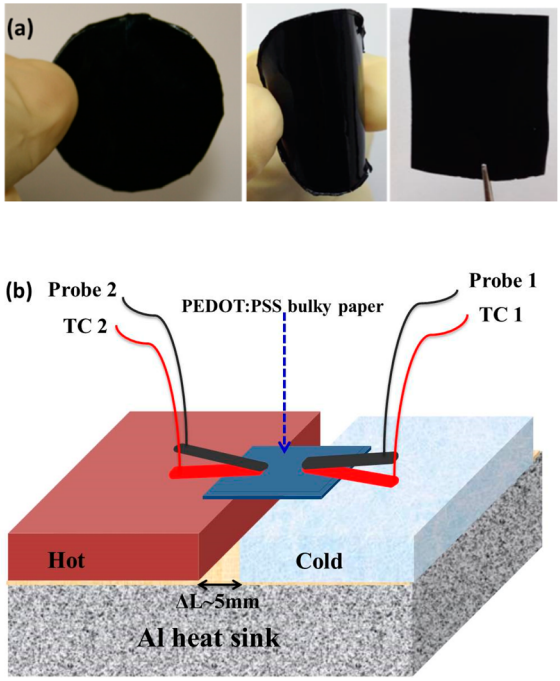

Figure 1. (a) Photographs of flexible PEDOT:PSS bulky papers in different shapes. (b) Schematic diagram of Seebeck coefficient measurement system.

3. RESULTS AND DISCUSSION

While there exists relatively more work on the thin film PEDOT:PSS for TEs, there is not much work on bulky papers. Lots of practical applications need thicker TE materials. Photographs of PEDOT:PSS bulky papers prepared by vacuum-assisted filtration are shown in Figure 1a. As can be clearly seen, the papers are large size, smooth, flexible, and cuttable to any shape making them ideal for integration into any shape for future applications. The Anodisc filter membrane can be easily peeled off after vacuum drying. When drying was done in atmospheric ovens, the filter membrane can be slowly peeled with the assistance of methanol or isopropanol. Filtration can also be easily done using nylon filter membrane. The thickness of the papers can easily be controlled by controlling the amount of PEDOT:PSS solution used for filtration. Here we have demonstrated the TE performances of these thick papers (~100 μm) while comparing with the thin films (~200 nm) where necessary.

The conductivity, Seebeck coefficient, and power factor (PF) of PEDOT:PSS papers are shown in Figure 2. The conductivity values are similar to our previous reports.[31−33] The average conductivities are 0.3, 640, 800, 1300, and 1900 S cm^{-1} for pristine, EG, PEG, methanol, and FA-treated papers, respectively. The Seebeck coefficient decreased from 32.3 μV K^{-1} for pristine to 21.4 μV K^{-1} for EG-treated paper. Then Seebeck coefficient showed only slight variation with increasing conductivity being 21.7, 21.1, and 20.6 μV K^{-1} for PEG, methanol, and FA-treated papers, respectively. Corresponding to these values, the PF is 0.03, 29.3, 37.7, 58, and 80.6 μW m^{-1} K^{-2} for pristine, EG, PEG, methanol, and FA-treated papers, respectively. The PF of FA-treated papers is among the highest reported for PEDOT:PSS. The reported Seebeck coefficient was 27.3 μV K^{-1} for EG-treated PEDOT:PSS films showing the same conductivity.[16] The lower Seebeck coefficient values of our papers should be attributed to the measurement system. To

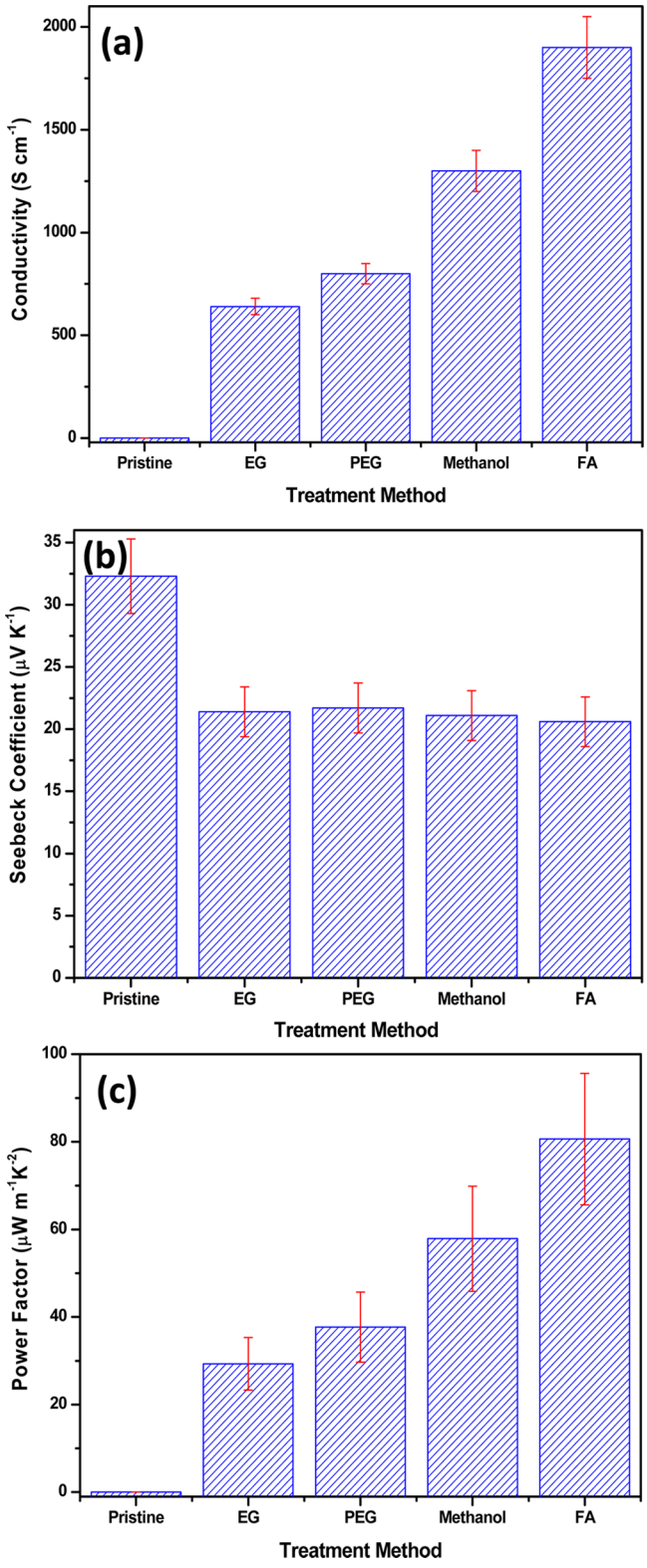

Figure 2. Thermoelectric properties of PEDOT:PSS bulky papers with different treatment methods: (a) electrical conductivity, (b) Seebeck coefficient, and (c) power factor.

assess this, we fabricated ~200 nm thin films. The Seebeck coefficient was even lower than the bulky papers being 28.4, 18.8, and 18.7 for μV K^{-1} for pristine, EG, and FA-treated films, respectively (Figure S3, Supporting Information). The highest PF for FA-treated thin films is only 66.4 μW m^{-1} K^{-2}. The

DOI: 10.1021/am507032e
ACS Appl. Mater. Interfaces 2015, 7, 94−100

reduced Seebeck coefficient for the thin films comes from contact problem (between the probe and thermocouple and thin film) as the probe and thermocouple we used were sheet types (to ensure wider area measurement), and it was difficult to make Ohmic contact as evidenced by higher sheet resistance than actually films have.

Previous reports on the effect of conductivity enhancement on Seebeck coefficient are somehow contradicting. Luo et al.[34] and Yee et al.[35] reported that Seebeck coefficient of PEDOT:PSS decreased slightly with increasing conductivity. However, Kim et al.[16] showed enhancement of Seebeck coefficient with enhanced conductivity when PEDOT:PSS was post treated with EG. Others controlled the oxidation level of PEDOT to optimize the power factor. In this case, electrical conductivity decreased a lot with increasing Seebeck coefficient.[36−39] Seebeck coefficient depends on the oxidation level of the polymer.[10] Secondary dopants, as used in our methods of treatment, do not change the oxidation level of PEDOT.[40] Secondary dopants increase the conductivity by increasing the mobility, carrier concentration, and morphology change of PDEOT:PSS films.[30,31] The slight decrease in Seebeck coefficient compared to the 4 orders of magnitude electrical conductivity enhancement is due to the increase in career concentration and mobility of treated samples. As reported in our previous works,[31−33] the carrier concentration increased from ∼10^{17} cm^{-3} for pristine PEDOT:PSS to ∼10^{21} cm^{-3} for the treated ones.

In PEDOT:PSS, PSS is used as the counterion, charge compensator, and template for polymerization of PEDOT, making it easily dispersible in water.[41] However, PSS is present in excess, insulator (nonionized dopant), and the main reason for the low conductivity of the commercial PEDOT:PSS. Selective removal of PSS is one of the mechanisms of conductivity enhancement.[27] The XPS spectra of the papers (Figure 3) shows that the amount of PSS decreased after treatment. The S (2p) peak at the binding energy of 167.8 eV corresponds to the sulfur signal from PSS, and the doublet peaks at 164.4 and 163.4 eV correspond to the sulfur signal from PEDOT both before and after treatment.[42] The amount of PSS decreased by as much as 62% for FA-treated papers, which is in agreement with that of thin films.[33] The relative decrease of PSS from the surface is due to the washing away of excess PSS for the methanol and FA treatments. For the EG and PEG-treated papers, there is no removal of PSS from the surface; rather, there is depletion of PSS layer from the surface, and the surface becomes PEDOT-rich. The amount of PSS removal/depletion from the PEDOT:PSS paper is in agreement with the respective conductivity enhancements. Secondary dopants with high dielectric constants induce screening effect between the positively charged PEDOT chains and negatively charged PSS chains, thus reducing the Coulombic interaction between them.[43] This in turn facilitates phase separation at the nanometer scale and the removal of PSS from the film. The removal of the insulator hygroscopic PSS from film surface will also improve its long-term stability.[31] There exist two types of PSS chains in PEDOT:PSS solution: complexed with PEDOT chains and "free PSS" chains, which act as a surfactant. It is the uncomplexed "free PSS" (nonionized) that is removed by film treatment, and its removal affects the thermoelectric property of PEDOT:PSS.[44]

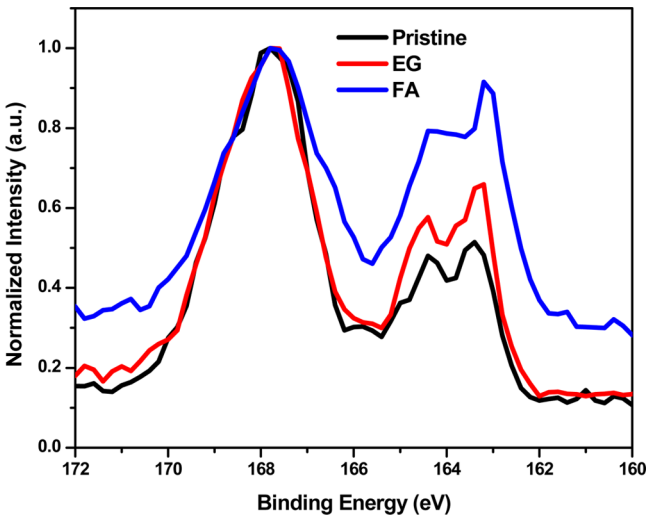

Figure 3. S(2p) XPS spectra of PEDOT:PSS bulky papers: pristine, treated with EG, and treated with FA.

PEDOT:PSS treatments with secondary dopants also change film morphologies, which again affect the electrical conductivity. The AFM images of thin films before and after treatment are shown in Figure 4. There is weak phase separation between PEDOT and PSS with more homogeneous and disconnected PEDOT chains for the pristine film. The phase image shows better phase separation between PEDOT and PSS chains with more fiber-like interconnected conductive PEDOT chains after film treatment. The degree of phase separation is related to the conductivity enhancement imparted. Interestingly, more or less the same phenomena is observed for the thick PEDOT:PSS bulky papers (Figure S4, Supporting Information). The depletion/removal of PSS leads to a three-dimensional conducting network of highly conductive PEDOT through which charge carriers travel further. The topographic AFM images indicate that the grain size of the particles increased after treatment. Bigger particles mean less particle boundaries in a given volume or area and hence few energy barriers for charge conduction.[45] A decrease in energy barrier will ease the charge hopping among the polymer chains, which is believed to be the dominant conduction mechanism in conducting polymers.[46] The thin films are quite smooth both before and after treatment. The rms (root-mean-square) roughness is 1.10, 1.28, 1.42, and 1.52 nm for pristine, treated with EG, methanol, and FA, respectively. The bulky papers are also reasonably smooth with rms roughness of 2.7, 3.25, 3.38, and 3.85 nm for pristine, treated with EG, methanol, and FA, respectively.

Figure 5 shows the Raman spectra of pristine and FA-treated PEDOT:PSS papers. The band between 1400 and 1500 cm^{-1} is due to $C_\alpha = C_\beta$ symmetric stretching vibration.[23] The 1430 cm^{-1} peak for the pristine paper is red-shifted to 1417 cm^{-1} after FA treatment. The same phenomenon was observed by Ouyang et al. when PEDOT:PSS was treated with EG.[47] The red shifting of the Raman spectra indicates that the resonant structure of PEDOT chain is changed from a benzoid structure with favorite coil conformation to quinoid structure with a favorite linear or expanded-coil structure. Both benzoid and quinoid structures may be present in the pristine; the benzoid structure will be transformed to quinoid structure after treatment making it quinoid dominated structure. PEDOT and PSS are held by Coulombic attractions and have coiled or core−shell structure due to repulsion between long PSS chains.[48] High dielectric constant solvents screen the ionic

DOI: 10.1021/am507032e
ACS Appl. Mater. Interfaces 2015, 7, 94−100

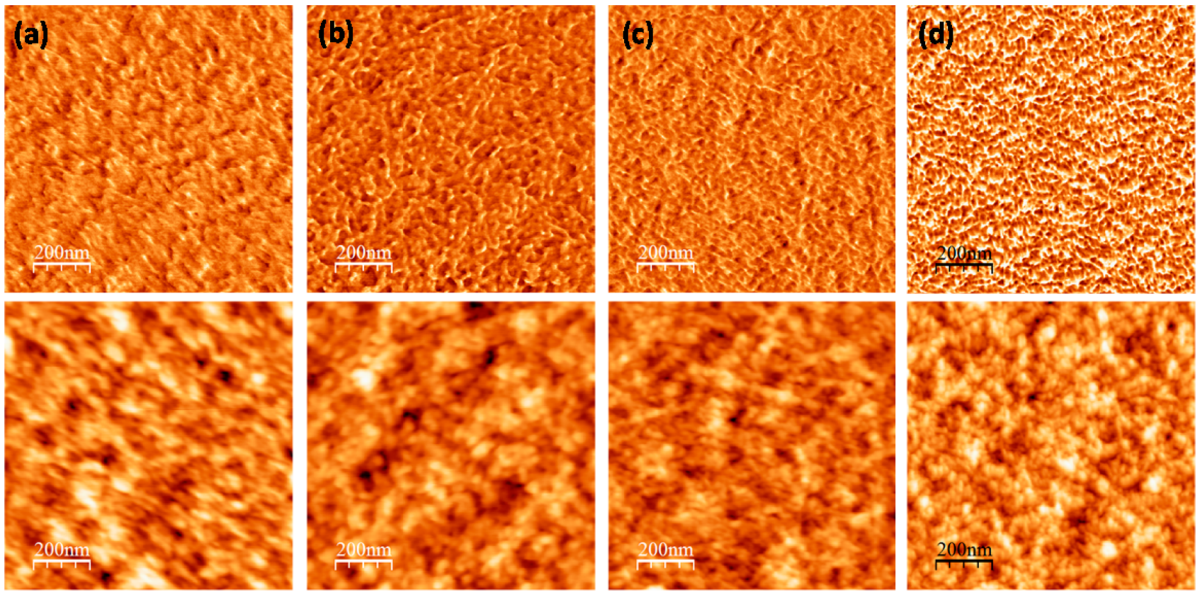

Figure 4. AFM images of PEDOT:PSS thin films: (a) pristine, treated with (b) EG, (c) methanol, and (d) formic acid. The upper images are phase images and the lower topographic. All images are 1 μm × 1 μm.

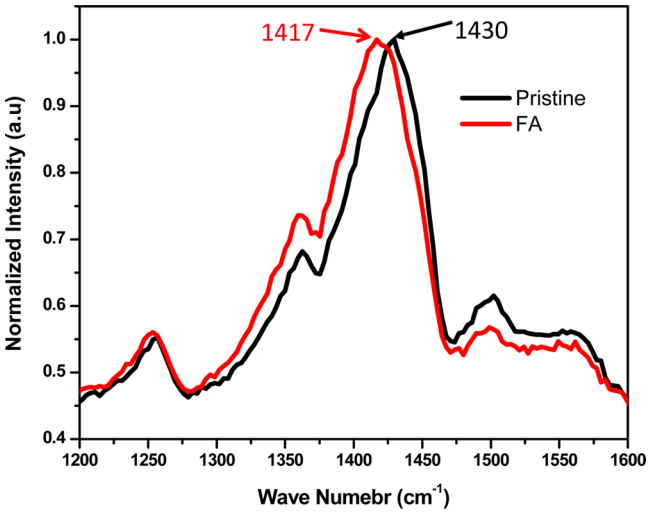

Figure 5. Raman spectra of pristine and FA-treated PEDOT:PSS bulky papers.

interaction between PEDOT and PSS leading to better phase separation between PEDOT and PSS and again giving the chance for PEDOT chain to be linearly oriented. There is only slight increase in the visible-IR absorption spectra after treatment (Figure S6, Supporting Information). The slight increase in absorption should be related to the more delocalized charge carriers, polarons, and bipolarons in PEDOT:PSS. Luo et al. observed a new broad absorption band in the visible and IR region after treatment with ionic liquid and attributed it to the change of PEDOT from bipolaron to polaron state, which increased the Seebeck coefficient.[34] However, there is no new absorption band in the visible or IR region after treatment in all of our treatments indicating that there is no such transformation.

For the inorganic TE materials, thermal conductivity increases with electrical conductivity, and thermal conductivity is reduced through introduction of nanostructures, which will act as phonon-scattering centers.[49] However, organic conductors do not obey the Wiedemann–Franz law, and there is weak correlation between electrical conductivity and thermal conductivity. The thermal conductivity of PEDOT:PSS is intrinsically low and is not much affected with increasing electrical conductivity. A recent report showed thermal conductivity of PEDOT:PSS decreased while electrical conductivity was enhanced through removal of PSS.[16,44] Using the thermal conductivity of 0.17 W $m^{-1}K^{-1}$,[50] the calculated ZT value at room temperature for FA-treated PEDOT:PSS bulky papers becomes ZT ≈ 0.14 (ZT ≈ 5.5 × 10^{-5}, 0.052, 0.066, 0.102 for pristine, EG, PEG, and methanol-treated bulky papers, respectively). Another method to directly measure the ZT value is the Harman method.[6,51] The Harman method is particularly useful for low thermal conductivity materials of small dimensions. Using the Harman method, the in-plane ZT value was 0.12, while the vertical ZT value was 0.32 (Figure S7, Supporting Information) for FA-treated samples. This ZT value is among the highest reported for PEDOT:PSS bulky papers. The in-plane ZT value is 0.05, 0.06, and 0.09, whereas the vertical ZT value is 0.13, 0.2, and 0.25 for EG, PEG, and methanol-treated PEDOT:PSS bulky papers, respectively. The difference in the in-plane and vertical ZT values is due to the anisotropic electrical and morphological properties of PEDOT:PSS.[52] The thermal conductivity is 0.18, 0.19, 0.19, and 0.2 for EG, PEG, methanol, and FA-treated bulky papers, respectively, when derived from the in-plane ZT values, which are in good agreement with the reported values.[44] However, we were not able to measure both the in-plane and vertical ZT values of pristine samples as the ZT value was too small and not detectable by our setup. The XRD patterns of PEDOT:PSS papers are same before and after treatment with no or very little crystallities embedded in the amorphous region (Figure S8, Supporting Information).

4. CONCLUSIONS

We have shown facile fabrication of flexible PEDOT:PSS bulky papers, which can be cut into any shape and are ideal for integration into any device shape. There was not much difference between the film properties of thin films and the

DOI: 10.1021/am507032e
ACS Appl. Mater. Interfaces 2015, 7, 94–100

bulky papers. The electrical conductivity of the papers was enhanced up to 1900 S cm^{-1} by FA treatment. The Seebeck coefficient was affected insignificantly with increasing electrical conductivity. The Seebeck coefficient and power factor were 20.6 $\mu V\ K^{-1}$ and 80.6 $\mu W\ m^{-1}\ K^{-2}$, respectively for FA-treated papers. A perpendicular ZT ≈ 0.32 at room temperature, which is among the highest values for PEDOT:PSS, was measured using Harman method. Enhancement of electrical conductivity, especially through selective removal of PSS, is a key strategy in enhancing the TE performance of PEDOT:PSS. This work demonstrates that PEDOT:PSS is promising for solution processable and flexible thermoelectrics especially with the recently reported high electrical conductivities. These kinds of freestanding flexible paper thermoelectrics will open up new possibilities in niche applications.

■ ASSOCIATED CONTENT

Supporting Information

Setup for PEDOT:PSS bulky paper preparation, schematic diagram of ZT measurement by Harman method, thermoelectric properties of PEDOT:PSS thin films, AFM images of bulky papers, absorption spectra of thin films, and graph of *V* versus *t* by Harman method for the vertical ZT measurement. This material is available free of charge via the Internet at http://pubs.acs.org.

■ AUTHOR INFORMATION

Corresponding Author

*Fax: 886-2-2787-3122. Phone: 886-2-2787-3183. E-mail: gchu@gate.sinica.edu.tw.

Notes

The authors declare no competing financial interest.

■ ACKNOWLEDGMENTS

The authors would like to thank Prof. Y.-C. Chang for the Hall Effect measurement system. This work was financially supported by Thematic Project of Academia Sinica (AS-100-TP-A05), and National Science Counsel (NSC102-2221-E-001-029-MY2), Taiwan.

■ REFERENCES

(1) Bell, L. E. Cooling, Heating, Generating Power, and Recovering Waste Heat with Thermoelectric Systems. *Science* **2008**, *321*, 1457−61.

(2) Tritt, T. M.; Subramanian, M. A. Thermoelectric Materials, Phenomena, and Applications: A Bird's Eye View. *MRS Bull.* **2006**, *31*, 188−198.

(3) Snyder, G. J.; Toberer, E. S. Complex Thermoelectric Materials. *Nat. Mater.* **2008**, *7*, 105−14.

(4) Chen, G.; Dresselhaus, M. S.; Dresselhaus, G.; Fleurial, J. P.; Caillat, T. Recent Developments in Thermoelectric Materials. *Int. Mater. Rev.* **2003**, *48*, 45−66.

(5) Liu, W.; Yan, X.; Chen, G.; Ren, Z. Recent Advances in Thermoelectric Nanocomposites. *Nano Energy* **2012**, *1*, 42−56.

(6) Venkatasubramanian, R.; Siivola, E.; Colpitts, T.; O'Quinn, B. Thin-Film Thermoelectric Devices with High Room-Temperature Figures of Merit. *Nature* **2001**, *413*, 597−602.

(7) Dubey, N.; Leclerc, M. Conducting Polymers: Efficient Thermoelectric Materials. *J. Polym. Sci., Part B: Polym. Phys.* **2011**, *49*, 467−475.

(8) He, M.; Qiu, F.; Lin, Z. Towards High-Performance Polymer-Based Thermoelectric Materials. *Energy Environ. Sci.* **2013**, *6*, 1352−1361.

(9) Poehler, T. O.; Katz, H. E. Prospects for Polymer-Based Thermoelectrics: State of the Art and Theoretical Analysis. *Energy Environ. Sci.* **2012**, *5*, 8110−8115.

(10) Bubnova, O.; Crispin, X. Towards Polymer-Based Organic Thermoelectric Generators. *Energy Environ. Sci.* **2012**, *5*, 9345−9362.

(11) Yue, R.; Chen, S.; Lu, B.; Liu, C.; Xu, J. Facile Electrosynthesis and Thermoelectric Performance of Electroactive Free-Standing Polythieno[3,2-B]Thiophene Films. *J. Solid State Electrochem.* **2011**, *15*, 539−548.

(12) Mateeva, N.; Niculescu, H.; Schlenoff, J.; Testardi, L. R. Correlation of Seebeck Coefficient and Electric Conductivity in Polyaniline and Polypyrrole. *J. Appl. Phys.* **1998**, *83*, 3111−3117.

(13) Yue, R.; Xu, J. Poly(3,4-Ethylenedioxythiophene) as Promising Organic Thermoelectric Materials: A Mini-Review. *Synth. Met.* **2012**, *162*, 912−917.

(14) Kaneko, H.; Ishiguro, T.; Takahashi, A.; Tsukamoto, J. Magnetoresistance and Thermoelectric Power Studies of Metal-Nonmetal Transition in Iodine-Doped Polyacetylene. *Synth. Met.* **1993**, *57*, 4900−4905.

(15) Zhang, Q.; Sun, Y.; Xu, W.; Zhu, D. Thermoelectric Energy from Flexible P3HT Films Doped with a Ferric Salt of Triflimide Anions. *Energy Environ. Sci.* **2012**, *5*, 9639−9644.

(16) Kim, G. H.; Shao, L.; Zhang, K.; Pipe, K. P. Engineered Doping of Organic Semiconductors for Enhanced Thermoelectric Efficiency. *Nat. Mater.* **2013**, *12*, 719−723.

(17) Wang, Y. Y.; Zhou, J.; Yang, R. G. Thermoelectric Properties of Molecular Nanowires. *J. Phys. Chem. C* **2011**, *115*, 24418−24428.

(18) Groenendaal, L.; Jonas, F.; Freitag, D.; Pielartzik, H.; Reynolds, J. R. Poly(3,4-Ethylenedioxythiophene) and Its Derivatives: Past, Present, and Future. *Adv. Mater.* **2000**, *12*, 481−494.

(19) Wang, P.-C.; Liu, L.-H.; Alemu Mengistie, D.; Li, K.-H.; Wen, B.-J.; Liu, T.-S.; Chu, C.-W. Transparent Electrodes Based on Conducting Polymers for Display Applications. *Displays* **2013**, *34*, 301−314.

(20) Wei, H.-Y.; Huang, J.-H.; Hsu, C.-Y.; Chang, F.-C.; Ho, K.-C.; Chu, C.-W. Organic Solar Cells Featuring Nanobowl Structures. *Energy Environ. Sci.* **2013**, *6*, 1192−1198.

(21) Xia, Y.; Sun, K.; Ouyang, J. Solution-Processed Metallic Conducting Polymer Films as Transparent Electrode of Optoelectronic Devices. *Adv. Mater.* **2012**, *24*, 2436−40.

(22) Fabretto, M. V.; Evans, D. R.; Mueller, M.; Zuber, K.; Hojati-Talemi, P.; Short, R. D.; Wallace, G. G.; Murphy, P. J. Polymeric Material with Metal-Like Conductivity for Next Generation Organic Electronic Devices. *Chem. Mater.* **2012**, *24*, 3998−4003.

(23) Ouyang, J.; Chu, C. W.; Chen, F. C.; Xu, Q.; Yang, Y. High-Conductivity Poly(3,4-Ethylenedioxythiophene):Poly(Styrene Sulfonate) Film and Its Application in Polymer Optoelectronic Devices. *Adv. Funct. Mater.* **2005**, *15*, 203−208.

(24) Badre, C.; Marquant, L.; Alsayed, A. M.; Hough, L. A. Highly Conductive Poly(3,4-Ethylenedioxythiophene):Poly (Styrenesulfonate) Films Using 1-Ethyl-3-Methylimidazolium Tetracyanoborate Ionic Liquid. *Adv. Funct. Mater.* **2012**, *22*, 2723−2727.

(25) Huang, J.-H.; Kekuda, D.; Chu, C.-W.; Ho, K.-C. Electrochemical Characterization of the Solvent-Enhanced Conductivity of Poly(3,4-Ethylenedioxythiophene) and Its Application in Polymer Solar Cells. *J. Mater. Chem.* **2009**, *19*, 3704−3712.

(26) Xia, Y.; Sun, K.; Ouyang, J. Highly Conductive Poly(3,4-Ethylenedioxythiophene):Poly(Styrene Sulfonate) Films Treated with an Amphiphilic Fluoro Compound as the Transparent Electrode of Polymer Solar Cells. *Energy Environ. Sci.* **2012**, *5*, 5325−5332.

(27) Kim, Y. H.; Sachse, C.; Machala, M. L.; May, C.; Müller-Meskamp, L.; Leo, K. Highly Conductive PEDOT:PSS Electrode with Optimized Solvent and Thermal Post-Treatment for ITO-Free Organic Solar Cells. *Adv. Funct. Mater.* **2011**, *21*, 1076−1081.

(28) MacDiarmid, A. G.; Epstein, A. J. The Concept of Secondary Doping as Applied to Polyaniline. *Synth. Met.* **1994**, *65*, 103−116.

(29) Bubnova, O.; Khan, Z. U.; Wang, H.; Braun, S.; Evans, D. R.; Fabretto, M.; Hojati-Talemi, P.; Dagnelund, D.; Arlin, J. B.; Geerts, Y. H.; Desbief, S.; Breiby, D. W.; Andreasen, J. W.; Lazzaroni, R.; Chen,

DOI: 10.1021/am507032e
ACS Appl. Mater. Interfaces 2015, 7, 94−100

W. M.; Zozoulenko, I.; Fahlman, M.; Murphy, P. J.; Berggren, M.; Crispin, X. Semi-Metallic Polymers. *Nat. Mater.* **2014**, *13*, 190−4.
(30) Wei, Q.; Mukaida, M.; Naitoh, Y.; Ishida, T. Morphological Change and Mobility Enhancement in PEDOT:PSS by Adding Co-Solvents. *Adv. Mater.* **2013**, *25*, 2831−2836.
(31) Alemu, D.; Wei, H.-Y.; Ho, K.-C.; Chu, C.-W. Highly Conductive PEDOT:PSS Electrode by Simple Film Treatment with Methanol for ITO-Free Polymer Solar Cells. *Energy Environ. Sci.* **2012**, *5*, 9662−9671.
(32) Mengistie, D. A.; Wang, P.-C.; Chu, C.-W. Effect of Molecular Weight of Additives on the Conductivity of PEDOT:PSS and Efficiency for ITO-Free Organic Solar Cells. *J. Mater. Chem. A* **2013**, *1*, 9907−9915.
(33) Mengistie, D. A.; Ibrahem, M. A.; Wang, P. C.; Chu, C. W. Highly Conductive PEDOT:PSS Treated with Formic Acid for ITO-Free Polymer Solar Cells. *ACS Appl. Mater. Interfaces* **2014**, *6*, 2292−9.
(34) Luo, J.; Billep, D.; Waechtler, T.; Otto, T.; Toader, M.; Gordan, O.; Sheremet, E.; Martin, J.; Hietschold, M.; Zahn, D. R. T.; Gessner, T. Enhancement of the Thermoelectric Properties of PEDOT:PSS Thin Films by Post-Treatment. *J. Mater. Chem. A* **2013**, *1*, 7576−7583.
(35) Yee, S. K.; Coates, N. E.; Majumdar, A.; Urban, J. J.; Segalman, R. A. Thermoelectric Power Factor Optimization in PEDOT:PSS Tellurium Nanowire Hybrid Composites. *Phys. Chem. Chem. Phys.* **2013**, *15*, 4024−4032.
(36) Bubnova, O.; Khan, Z. U.; Malti, A.; Braun, S.; Fahlman, M.; Berggren, M.; Crispin, X. Optimization of the Thermoelectric Figure of Merit in the Conducting Polymer Poly(3,4-Ethylenedioxythiophene). *Nat. Mater.* **2011**, *10*, 429−433.
(37) Park, T.; Park, C.; Kim, B.; Shin, H.; Kim, E. Flexible PEDOT Electrodes with Large Thermoelectric Power Factors to Generate Electricity by the Touch of Fingertips. *Energy Environ. Sci.* **2013**, *6*, 788−792.
(38) Park, H.; Lee, S. H.; Kim, F. S.; Choi, H. H.; Cheong, I. W.; Kim, J. H. Enhanced Thermoelectric Properties of PEDOT:PSS Nanofilms by a Chemical Dedoping Process. *J. Mater. Chem. A* **2014**, *2*, 6532−6539.
(39) Massonnet, N.; Carella, A.; Jaudouin, O.; Rannou, P.; Laval, G.; Celle, C.; Simonato, J.-P. Improvement of the Seebeck Coefficient of PEDOT:PSS by Chemical Reduction Combined with a Novel Method for Its Transfer Using Free-Standing Thin Films. *J. Mater. Chem. C* **2014**, *2*, 1278−1283.
(40) Ouyang, J. Secondary Doping" Methods to Significantly Enhance the Conductivity of PEDOT:PSS for Its Application as Transparent Electrode of Optoelectronic Devices. *Displays* **2013**, *34*, 423−436.
(41) Kirchmeyer, S.; Reuter, K. Scientific Importance, Properties and Growing Applications of Poly(3,4-Ethylenedioxythiophene). *J. Mater. Chem.* **2005**, *15*, 2077−2088.
(42) Crispin, X.; Jakobsson, F. L. E.; Crispin, A.; Grim, P. C. M.; Andersson, P.; Volodin, A.; van Haesendonck, C.; Van der Auweraer, M.; Salaneck, W. R.; Berggren, M. The Origin of the High Conductivity of Poly(3,4-Ethylenedioxythiophene)−Poly-(Styrenesulfonate) (PEDOT−PSS) Plastic Electrodes. *Chem. Mater.* **2006**, *18*, 4354−4360.
(43) Kim, J. Y.; Jung, J. H.; Lee, D. E.; Joo, J. Enhancement of Electrical Conductivity of Poly(3,4-Ethylenedioxythiophene)/Poly(4-Styrenesulfonate) by a Change of Solvents. *Synth. Met.* **2002**, *126*, 311−316.
(44) Lee, S. H.; Park, H.; Son, W.; Choi, H. H.; Kim, J. H. Novel Solution-Processable, Dedoped Semiconductors for Application in Thermoelectric Devices. *J. Mater. Chem. A* **2014**, *2*, 13380−13387.
(45) Na, S.-I.; Kim, S.-S.; Jo, J.; Kim, D.-Y. Efficient and Flexible ITO-Free Organic Solar Cells Using Highly Conductive Polymer Anodes. *Adv. Mater.* **2008**, *20*, 4061−4067.
(46) Aleshin, A.; Kiebooms, R.; Menon, R.; Heeger, A. J. Electronic Transport in Doped Poly (3,4-Ethylenedioxythiophene) near the Metal-Insulator Transition. *Synth. Met.* **1997**, *90*, 61−68.
(47) Ouyang, J.; Xu, Q.; Chu, C.-W.; Yang, Y.; Li, G.; Shinar, J. On the Mechanism of Conductivity Enhancement in Poly(3,4-Ethylenedioxythiophene):Poly(Styrene Sulfonate) Film through Solvent Treatment. *Polymer* **2004**, *45*, 8443−8450.
(48) Lang, U.; Müller, E.; Naujoks, N.; Dual, J. Microscopical Investigations of PEDOT:PSS Thin Films. *Adv. Funct. Mater.* **2009**, *19*, 1215−1220.
(49) Minnich, A. J.; Dresselhaus, M. S.; Ren, Z. F.; Chen, G. Bulk Nanostructured Thermoelectric Materials: Current Research and Future Prospects. *Energy Environ. Sci.* **2009**, *2*, 466.
(50) Jiang, F.-X.; Xu, J.-K.; Lu, B.-Y.; Xie, Y.; Huang, R.-J.; Li, L.-F. Thermoelectric Performance of Poly(3,4-Ethylenedioxythiophene): Poly(Styrenesulfonate). *Chin. Phys. Lett.* **2008**, *25*, 2202.
(51) Harman, T. C.; Cahn, J. H.; Logan, M. J. Measurement of Thermal Conductivity by Utilization of the Peltier Effect. *J. Appl. Phys.* **1959**, *30*, 1351−1359.
(52) Nardes, A. M.; Kemerink, M.; Janssen, R. A. J.; Bastiaansen, J. A. M.; Kiggen, N. M. M.; Langeveld, B. M. W.; van Breemen, A. J. J. M.; de Kok, M. M. Microscopic Understanding of the Anisotropic Conductivity of PEDOT:PSS Thin Films. *Adv. Mater.* **2007**, *19*, 1196−1200.

DOI: 10.1021/am507032e
ACS Appl. Mater. Interfaces 2015, 7, 94−100